Available online at www.sciencedirect.com
ScienceDirect
Journal of Catalysis 254 (2008) 39–48
JOURNAL OF CATALYSIS
www.elsevier.com/locate/jcat

Highly sulfur-tolerant Pt/$Ce_{0.8}Gd_{0.2}O_{1.9}$ catalyst for steam reforming of liquid hydrocarbons in fuel cell applications

Yong Lu *, Jinchun Chen, Ye Liu, Qingsong Xue, Mingyuan He

Shanghai Key Laboratory of Green Chemistry and Chemical Processes, Department of Chemistry, East China Normal University, Shanghai 200062, China

Received 2 August 2007; revised 22 November 2007; accepted 23 November 2007

Available online 21 December 2007

Abstract

A sulfur-tolerant Pt catalyst has been developed for fuel processors being developed for use with fuel cells, using a fluorite-type $Ce_{0.8}Gd_{0.2}O_{1.9}$ support. The catalyst calcination temperature is crucial to ensure the maintenance of sulfur tolerance. The catalyst calcined at 800 °C retained its activity and selectivity for entire 100-h test period in the steam reforming of iso-octane with ⩾300 μg/g of sulfur, whereas the catalyst calcined at 600 °C obviously lost activity in this course. *In situ* diffuse reflectance infrared Fourier transform spectroscopy (DRIFTS) for CO and CO/H_2S adsorption was performed to characterize the nature of the Pt sites and to evaluate their ability to tolerate sulfur. Strongly electron-deficient Pt sites, evidenced by a CO adsorption band at ν_{max} 2104–2108 cm^{-1}, were immune to sulfur poisoning and were uniformly formed with the calcination at 800 °C. In addition, thiophene sulfur was completely converted into H_2S and likely complied with a redox mechanism.

Keywords: Steam reforming; Hydrocarbon; Hydrogen production; Sulfur tolerance; Ceria; Pt catalyst; Fuel cell; *In situ* DRIFTS

1. Introduction

Fuel cells have been emerged as promising devices for clean and efficient generation of power for global energy needs. The proton-exchanged membrane fuel cell (PEMFC) is a preferred fuel cell technology for many transportation applications [1,2]. Until a widespread hydrogen refueling infrastructure exists, on-board reformation technologies are needed to convert high-energy density commercial-grade liquid hydrocarbon fuels into hydrogen for PEMFCs. A significant challenge facing this effort is the development of high-efficiency fuel processing catalysts that must be active, selective, durable, and tolerant to sulfur and coke formation.

For higher hydrocarbons, the reforming catalysts typically include such metals as Pt, Rh, Ru, and Ni deposited or incorporated into carefully engineered oxide supports, such as ceria-containing oxides [3–5]. Significant improvements in reforming catalysts in terms of thermal stability, mechanical robustness, activity/selectivity, and coke resistance have been achieved by using active metals, carefully tailoring supports, and carefully selecting textural/structural promoters and loadings. Nevertheless, the sulfur tolerance of reforming catalysts remains a particularly challenging area.

Recently, a few special sulfur-tolerant catalysts have been mentioned in the open literature, albeit with confidential formulations [3–5]. A specific supported precious metal catalyst with a proprietary formulation, able to cope with 100 ppm sulfur, has been developed by Johnson Matthey for steam reforming (SR) of higher hydrocarbons [3]. A proprietary catalyst of bimetallic compound supported on high-surface-area Al_2O_3 treated with an oxide with oxygen ion-conducting properties and sulfur resistance comparable to that of the Johnson Matthey catalyst has been developed by InnovaTek [4]. The U.S. Department of Energy's Argonne National Laboratory has developed a highly sulfur-tolerant Pt/dope-ceria autothermal reforming (ATR) catalyst with proprietary formulations, but only initial reaction results in the presence of sulfur have been reported [5]. Recently, bimetallic Rh–Ni catalysts loaded on CeO_2-modified Al_2O_3 support have been reported to be successful for steam reforming of a JP-8 jet fuel with 22 ppm of sulfur for 72 h with >95% conversion, with Ni acting as a protective and sacrificial metal for Rh, thereby leading to much greater sulfur tolerance [6].

* Corresponding author. Fax: +86 21 62233424.
E-mail address: ylu@chem.ecnu.edu.cn (Y. Lu).

0021-9517/$ – see front matter
doi:10.1016/j.jcat.2007.11.015

A novel approach that combines the concepts of shape selectivity and hydrogen spillover has been developed to design sulfur-tolerant hydrogenation catalysts; the Pt particles entrapped in the KA-zeolite cages have shown resistance to sulfur poisoning because the reduced pore opening can successfully prevent H_2S molecules from attacking Pt particles while allowing hydrogen molecules to enter freely [7]. Despite these advances, developing a reforming catalyst with significantly improved resistance to sulfur remains a worthwhile goal, because retail gasoline generally contains 50–300 μg/g of sulfur (>300 μg/g in China). In addition, the confidentiality of currently available catalyst formulations greatly restricts comprehensive research and development activities aimed at further improving the sulfur resistance of SR catalysts for use in PEMFCs.

Particular attention is currently focused on materials with oxygen ion-conducting properties, especially metal-doped ceria [8–10]. Ceria loaded with promoter metals (e.g., Pt, Rh, Pd) are widely used for various catalytic applications, including three-way catalysts [11], selective oxidation or dehydrogenation of organic compounds [12,13], solid fuel cells [14], CO oxidation [9], the water–gas shift reaction [15], and membranes for efficient syngas generation by the partial oxidation of methane [8,16]. Many of these applications depend on the high oxygen ion conductivity and oxygen storage capacity of ceria, which can be further promoted by doping with other rare earth elements, such as Gd, Pr, and Sm. In addition, Gd-doped ceria dioxide shows significantly improved thermal stability compared with neat ceria, an important characteristic in applications in catalysis at elevated temperatures and use as an electrolyte in solid oxide fuel cells (SOFCs) [8,17]. Numerous studies also have been devoted to ceria-containing catalysts (for, e.g., CO oxidation), investigating chemisorptive and structural properties as well as surface states under reaction conditions [18]. Strong Pt–CeO_2 interactions have been demonstrated, and the chemical and electronic effects associated with onset of the strong Pt–CeO_2 interaction have been revealed, mainly in relation to the reduction temperature [18]. At present, however, development of sulfur-tolerant SR catalysts using the oxygen ion-conducting oxides as supports or catalyst additives is a relatively new area, and we know of only limited published data [3–5].

Herein we report a Pt catalyst supported on a fluorite-type $Ce_{0.8}Gd_{0.2}O_{1.9}$ (CeGdO) oxide that was found to be able to cope with ⩾300 μg/g sulfur in the SR of iso-octane. The fluorite-type CeGdO oxide support were prepared by citric acid sol–gel method, and Pt was highly dispersed onto the oxide surface by an incipient wetness impregnation (IWI) method. To gain insight into the nature of Pt sites and their ability to tolerate sulfur, the catalysts were characterized by means of H_2 temperature-programmed reduction (H_2-TPR) and *in situ* diffuse reflectance infrared Fourier transform spectroscopy (DRIFTS) for CO and CO/H_2S adsorption. In addition, a redox mechanism for conversion of thiophene into H_2S was evaluated. We anticipate that our report will initiate attempts to gain more insight into the reaction chemistry of sulfur transformation and the nature of sulfur tolerance of the Pt/CeGdO catalyst.

2. Experimental

2.1. Catalyst preparation

The fluorite-type CeGdO oxide was synthesized by a citric acid sol–gel method. Stoichiometric quantities of $Ce(NO_3)_3 \cdot 6H_2O$ and $Gd(NO_3)_2 \cdot 6H_2O$ were dissolved in deionized water to produce an aqueous solution with a total metal concentration of 0.6 mol/L. To this solution, an aqueous solution saturated with citric acid mixed with ethylene glycol (3:2 weight ratio of citric acid to ethylene glycol) was added dropwise at room temperature under vigorous stirring, ensuring a [M]/[citric acid] ratio of 1. The resulting mixture was subsequently evaporated at 80–90 °C to create a sol–gel of organic complex on a hot plate with a magnetic agitator, dried at 110 °C overnight, calcined at 500 °C in air for 2 h, crushed, and sieved into 60- to 100-mesh particulates. Pt was then placed onto the surface of as-made CeGdO oxide particulates by IWI of $H_2PtCl_6 \cdot 6H_2O$ to a Pt loading of 1.5 wt%. The products thus obtained were dried at 110 °C overnight and calcined in air at 600, 800, and 1000 °C for 2 h; these products are designated Pt/CeGdO-600, -800, and -1000, respectively. For comparative studies, both 10 wt% Ni/CeGdO [with $Ni(NO_3)_2 \cdot 6H_2O$ as a precursor] and 1.5 wt% Pt/Al_2O_3 (with active Al_2O_3 as a support: 60–100 mesh, SA of 270 m^2/g) catalysts also were prepared by IWI and subsequently calcined in air at 800 and 550 °C for 2 h; these are designated Ni/CeGdO and Pt/Al_2O_3, respectively.

2.2. Catalytic reaction tests

The SR of iso-octane was carried out with 1.0 g of catalyst particulates packed into a fixed-bed continuous-flow quartz tube reactor (19 mm i.d.) and heated by a tubular furnace. The Pt catalysts were directly heated and exposed to a feed stream with no prereduction with hydrogen. Iso-octane and water were controlled separately by two exact liquid pumps. A HP 6850 gas chromatograph equipped with a thermal conductivity detector and a 30-m AT-plot capillary column was used to analyze H_2, N_2, CO, CO_2, and C_1–C_3 hydrocarbons in the effluent, using an He carrier. The column temperature was programmed from 40 to 160 °C at a ramp of 30 °C/min with a hold time of 3 min at each of the initial and final temperatures. Conversion and product composition were calculated by the N_2 internal standard method as described previously [19], using a N_2 flow rate of 10 mL/min.

A Varian CP 3800 gas chromatograph equipped with a pulsed-flame photometric detector (PFPD) and a 60-m CP-Sil 8 CD capillary column and a HP 6890/5973N gas chromatograph–mass spectrometer with a HP-1 capillary column were used to analyze the S-containing product in the effluent gas. A WK-2D microcoulomb sulfur analyzer (Jiangsu Electroanalysis, China) and a Nicolet Nexus 670 Fourier transform infrared (FTIR) spectrometer were used to determine the sulfur form and content on the reacted catalysts.

2.3. Catalyst characterization

Brunauer–Emmett–Teller (BET) surface area measurements were obtained using a Quantromn Autosorb 3B gas adsorption analyzer, using N_2 adsorption at its boiling temperature. A sample loading of ∼0.25 g was used in each trial.

X-ray diffraction (XRD) patterns were obtained with a Bruker D8 Advance diffractometer, using Cu$K\alpha$ radiation at an acceleration voltage of 40 kV. The step scans were obtained over a 2θ range of 20–90° in steps of 0.02°, and the intensity data for each scan were collected for 10 s.

H_2-TPR experiments were carried out with a commercial chemisorption instrument (Quantromn ChemBET 3000) equipped with a thermal conductivity detector. In each trial, 0.2 g of sample was used. Before the H_2-TPR measurement, the sample was pretreated for 30 min at 500 °C in a gas mixture of 3% O_2 in He at a flux rate of 30 mL/min, cooled to room temperature, and then flushed thoroughly with ultrapure Ar. After this pretreatment, H_2-TPR was performed with a gas mixture of 5% H_2 in Ar. In all cases, the flow rate of gas fed to the reactor was maintained at 30 mL/min while the temperature of sample was ramped at 10 °C/min. CO-pulse adsorption experiments also were carried out with this chemisorption instrument to determine the Pt dispersion by assuming a CO/Pt ratio of 1. The sample was prereduced with 5% H_2 in Ar at 350 °C for 2 h, then cooled to room temperature in pure He. Subsequently, a sample of 10% CO in He was pulsed, with a pulse volume of 500 μL, to the reactor every 3 min until the CO peak intensity remained unchanged.

In situ DRIFTS spectra for CO adsorption and CO/H_2S coadsorption were recorded with a Nicolet Nexus 670 FTIR spectrometer equipped with a MCT/B detector. A total of 128 scans were obtained for each spectrum with a resolution of 4 cm^{-1}. A high-temperature DRIFTS reactor cell with a ZnSe window (Nexus Smart Collector) connected to a purging/adsorption gas control system was used for *in situ* adsorption measurements. Powder catalysts were packed into the sample vessel of the reactor cell and prereduced with H_2 at 350 °C for 1 h if not specified otherwise, followed by Ar purging at 350 °C for 1 h and cooling in Ar flow to room temperature. Spectra for CO adsorption were recorded when a 10% CO/Ar flow of 20 mL/min was switched to pass through the DRIFTS reactor cell packed with prereduced samples at room temperature for 30 min, followed by Ar purging at room temperature for 1 h. After the CO adsorption experiments, the catalyst surfaces were exposed to H_2S by feeding 1% H_2S/Ar at a flow rate of 2 mL/min (together with an Ar flow of 20 mL/min) into the DRIFTS reactor cell for 10 min; then the spectra were rerecorded after Ar purging at room temperature for 1 h.

3. Results and discussion

3.1. Reactivity with respect to SR of iso-octane in the absence of sulfur

Preliminary experiments were carried out to study the effect of weight hourly space velocity (WHSV) of iso-octane and the catalyst calcination temperature on the reactivity of Pt/CeGdO catalyst for the SR of iso-octane in the absence of sulfur at 750 °C with a steam/C molar ratio of 3. Iso-octane conversion and product composition versus the WHSV of iso-octane and the catalyst calcination temperature are presented in Fig. 1 and Table 1, respectively. As shown in Fig. 1, over the Pt/CeGdO-800 catalyst, the optimal iso-octane WHSV was at 0.8–1.0 h^{-1}; nearly 100% conversion was obtained with a reformate composition of ∼72% H_2, ∼15% CO_2, ∼12% CO, and trace CH_4. Increasing the iso-octane WHSV from 0.8 to 3.4 h^{-1} obviously decreased the conversion to ∼85%, accompanied by slight decreases in the concentrations of H_2 to ∼70%

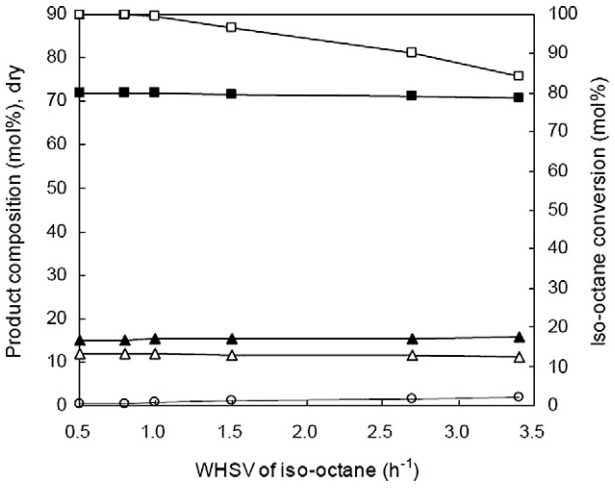

Fig. 1. Conversion and product composition versus WHSV of iso-octane over the Pt/CeGdO-800 at 750 °C and 0.1 MPa with a steam/C ratio of 3. (□) Iso-octane conversion; (■) H_2; (▲) CO_2; (△) CO; (○) CH_4.

Table 1
Effect of the calcination temperature of Pt/CeGdO catalysts on conversion and product composition for the SR of iso-octane[a]

Calcination temperature (°C)	S_{BET} (m^2/g)	Pt dispersion (%)	Iso-octane conversion (mol%)	Product composition (mol%), dry			
				H_2	CO	CO_2	CH_4
600	57	63	99.7	71.7	12.4	15.6	0.3
800	39	59	99.1	72.4	12.1	15.3	0.2
1000	10	15	80.0	69.1	11.7	16.2	3.0[c]
Equilibrium[b]			100	72	13	15	Trace

[a] Each reaction condition was run for 2 h, during which the experimental data were collected; reaction conditions: steam/C molar ratio of 3.0, iso-octane WHSV of 0.8 h^{-1}, 750 °C, 0.1 MPa, catalyst of 1.0 g.

[b] Total C_1–C_2 product fraction wherein CH_4 fraction was 2.5%.

[c] At 750 °C and steam/C molar ratio of 3.6 (from Ref. [3]).

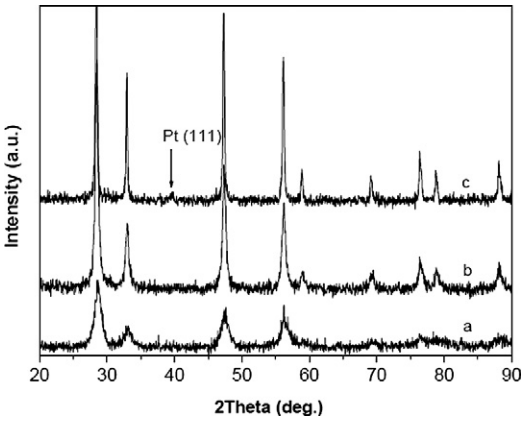

Fig. 2. XRD patterns of Pt/CeGdO catalysts calcined for 2 h at (a) 600, (b) 800, and (c) 1000 °C.

and of CO to ∼11% but slight increases in the concentrations of CO_2 to ∼16% and of CH_4 to ∼2% (Fig. 1). As shown in Table 1, the iso-octane conversion of >99% and the thermodynamic equilibrium product composition were achieved over both the Pt/CeGdO-600 and Pt/CeGdO-800 catalysts at 750 °C with an iso-octane WHSV of 0.8 h^{-1}, due to these catalysts' good Pt dispersion (63 and 59%, respectively) and large surface area (57 and 39 m^2/g, respectively).

Fig. 2 shows the XRD patterns of the Pt/CeGdO catalysts calcined at various temperatures. The CeGdO supports provided a sintering tendency with increasing calcination temperature, but obvious sintering of Pt occurred only at a calcination temperature of 1000 °C. This was consistent with the trends in BET surface areas and Pt dispersion against the calcination temperature, as displayed in Table 1. A high calcination temperature of 1000 °C caused severe sintering of both the Pt particles (Pt dispersion of 15%) and CeGdO oxides, thereby leading to its low iso-octane conversion of 80% while yielding more C_1–C_2 hydrocarbons from the pyrolysis of iso-octane (Table 1).

It should be noted, however, that the decrease in iso-octane conversion of the Pt/CeGdO-1000 catalyst was not proportional to the decrease in Pt dispersion when compared with the Pt/CeGdO-800 catalyst: 80% versus ∼100% for conversion and 15% versus 53% for Pt dispersion (Table 1). This suggests that the Pt–CeGdO interface might be more active than the Pt particle surface for this reaction process. Actually, the unique Pt–CeO_2 interface has been shown to offer high activity and excellent selectivity for the water–gas shift reaction [20] and preferential oxidation of the CO reaction [9]. Nevertheless, calcination at 1000 °C likely caused the marked suppression of chemisorption of CO on the Pt found in reduction treatment at ⩾500 °C [18,21–23]. If this were to occur on the Pt/CeGdO-1000 catalyst, then Pt dispersion estimated by CO chemisorption would be lower yet, resulting in an iso-octane conversion–Pt dispersion mismatch.

3.2. Sulfur tolerance of Pt/CeGdO catalysts for SR of iso-octane

The Pt/CeGdO-600 and Pt/CeGdO-800 catalysts were selected for a longer-term test of the SR of iso-octane with

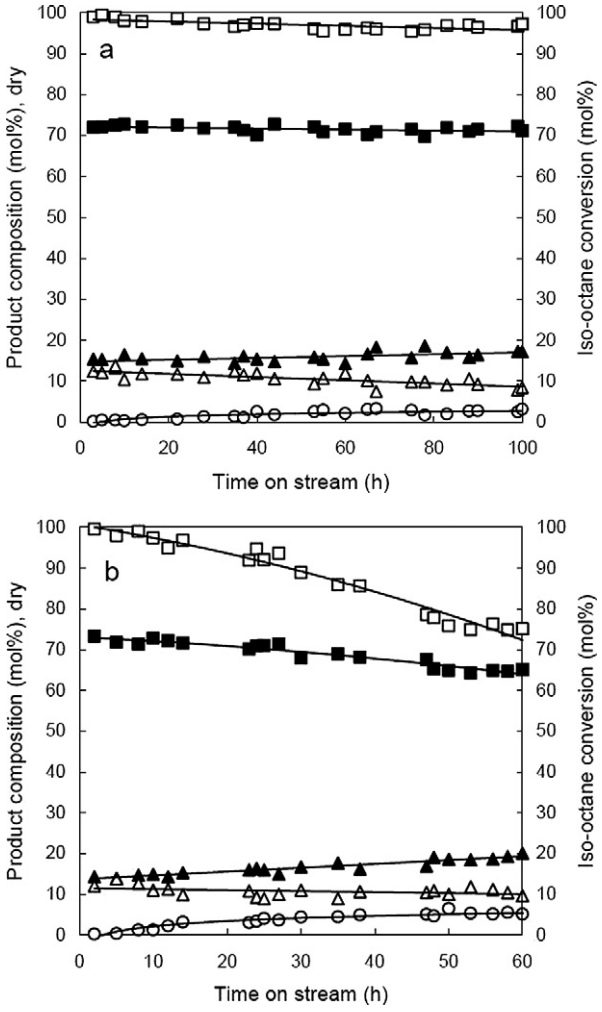

Fig. 3. Conversion and product composition for longer-term test of the SR of iso-octane with 300 μg/g sulfur, using (a) Pt/CeGdO-800 and (b) Pt/CeGdO-600. Reaction conditions: 750 °C, 0.1 MPa, steam/C ratio of 3 and iso-octane WHSV of 1.0 h^{-1}. (□) Iso-octane conversion; (■) H_2; (▲) CO_2; (△) CO; (○) CH_4.

300 μg/g sulfur, because both of them were active and selective in the SR of neat iso-octane. Thiophene was used as sulfur source. Fig. 3 shows the conversion of iso-octane and the product composition over a longer-term test. Clearly, the Pt/CeGdO-800 catalyst maintained its activity and selectivity for the entire 100-h test, whereas the Pt/CeGdO-600 catalyst lost its activity obviously with the time on stream. Over the Pt/CeGdO-800 catalyst, the iso-octane conversion was sustained at >95% with the hydrogen concentration of ∼72% throughout the test, whereas the concentration of CH_4 was low, typically <3%. In contrast, over the Pt/CeGdO-600 catalyst, the iso-octane conversion was decreased continuously from nearly 100% to ∼75%, accompanied by a obvious decrease in the H_2 concentration from ∼72 to ∼65%, as well a continuous increase in the CH_4 concentration to >5% and obvious formation of the C_2 hydrocarbons (∼0.8%) within 60 h.

To clarify this significant difference in the reactivity between the Pt/CeGdO-600 and Pt/CeGdO-800 catalysts during the SR of iso-octane with 300 μg/g sulfur, longer-term tests of these

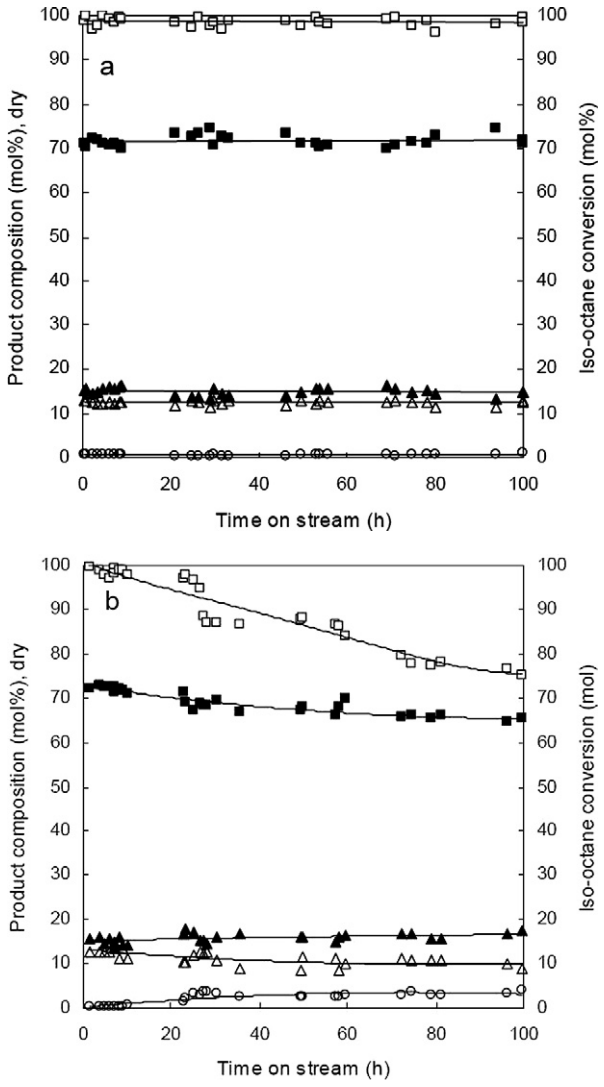

Fig. 4. Conversion and product composition for 100-h test of the SR of neat iso-octane, using (a) Pt/CeGdO-800 and (b) Pt/CeGdO-600. Reaction conditions: 750 °C, 0.1 M Pa, steam/C molar ratio of 3 and iso-octane WHSV of 1.0 h^{-1}. (□) Iso-octane conversion; (■) H_2; (▲) CO_2; (△) CO; (○) CH_4.

both catalysts in the absence of sulfur were carried out to explore the possible reasons. Fig. 4 shows the conversion of iso-octane and the product composition over a 100-h test. As can be seen, the Pt/CeGdO-800 catalyst provided nearly 100% conversion and a product composition comparable to that in the presence of 300 μg/g sulfur for the entire 100-h test, further confirming its excellent ability to tolerate sulfur. In agreement with a previous report on the formation of more CH_4 in the SR of iso-octane with sulfur [4], over the Pt/CeGdO-800 catalyst, the CH_4 concentration was increased from ∼1% in the absence of sulfur (Fig. 4) to ∼3% in the presence of sulfur over the entire 100-h test (Fig. 3). Likewise, the Pt/CeGdO-600 catalyst lost activity with time on stream in the absence of sulfur, but more slowly than it did in the presence of sulfur. The iso-octane conversion decreased continuously from nearly 100% to ∼85% in the absence of sulfur over the 100-h test and to ∼75% in the presence of 300 μg/g sulfur over just the 60-h test; the H_2 concentration decreased from ∼72 to 70% in the absence of sulfur and from ∼72 to ∼65% in the presence of 300 μg/g sulfur, whereas the CH_4 concentration increased to ∼3 and >5%, respectively (Figs. 3 and 4). The faster deactivation in the presence of sulfur was in good agreement with the fact that a type of Pt site existed that was unable to avoid sulfur attack on the Pt/CeGdO-600 catalyst by *in situ* DRIFTS for CO/H_2S co-adsorption (in the posterior section). The XRD measurements indicate that severe sintering of the CeGdO oxide occurred over the Pt/CeGdO-600 catalyst during the 100-h test in the absence of sulfur, whereas the used Pt/CeGdO-800 catalyst provided XRD patterns and signal intensities quite similar to those of the fresh one (not shown). The foregoing results suggest that both the sulfur poisoning and the poor thermal stability degraded the performance of Pt/CeGdO-600 during the SR of iso-octane with 300 μg/g sulfur.

The BET surface areas of the Pt/CeGdO-800 and Pt/CeGdO-600 catalysts were decreased to 18 and 12 m^2/g, respectively, after the sulfur tolerance tests as shown in Fig. 3. Fig. 5 shows the XRD patterns of the Pt/CeGdO-800 and Pt/CeGdO-600 catalysts before and after the sulfur tolerance tests as shown in Fig. 3. Although severe sintering of Pt did not occur due to the absence of detectable Pt(111) XRD peak for both used catalysts, severe crystallization of the oxide support during the reaction occurred for the Pt/CeGdO-600 but not for the Pt/CeGdO-800. The foregoing results indicate that the calcination treatment at 800 °C in air endowed the Pt/CeGdO with highly stable oxide crystals that might be characteristically indispensable for ensuring sulfur tolerance.

The SR of iso-octane with 500 μg/g of sulfur using the Pt/CeGdO-800 catalyst also was conducted for a 100-h test. Fig. 6 shows the conversion of iso-octane and the product composition versus time on stream. The conversion of iso-octane was slowly decreased to ∼90% within ∼50 h and then sustained at ∼90% throughout the 100-h test, accompanied by an increase in CH_4 concentration from ∼0.5 to ∼5% and in CO_2 concentration from ∼15 to ∼17%, as well a decrease in CO concentration from ∼12 to ∼10%. The H_2 concentration dropped slightly from ∼72 to ∼70% in this course. Whereas the severe crystalization of CeGdO support did not occur for the Pt/CeGdO-800 catalyst during the 100-h test, collapse of the piled pore of the CeGdO support could not be avoided due to the observation of the reduction of BET surface area in this course. This probably buried some active sites inside the collapsed pores, thereby leading to a decrease in iso-octane conversion. Interestingly, the BET surface area of the Pt/CeGdO-800 catalyst decreased from 39 to 19 m^2/g when this catalyst was calcinated at 750 °C in air for 50 h, but prolonging the calcination time to 100 h produced just another 2 m^2/g decrease in BET surface area. This might be the main reason why the iso-octane conversion was maintained at ∼90% after a slow decrease within first 50-h run.

For comparison, both the Pt/Al_2O_3 and Ni/CeGdO catalysts also were tested under the compatible reaction conditions for the SR of iso-octane with 300 μg/g of sulfur. Both of the catalysts had good activity/selectivity initially, but quickly lost their reactivity (Fig. 7). The CH_4 concentration increased up to >15% in 3 h or less, whereas the hydrogen concentration dropped by >10% within the same time period. In contrast, in

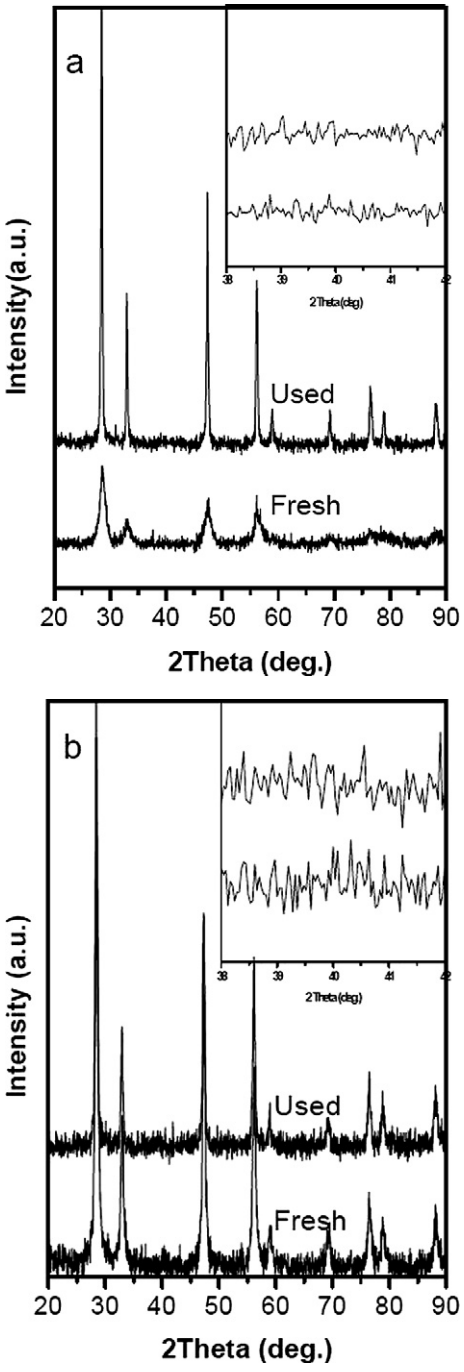

Fig. 5. XRD patterns of catalysts of (a) Pt/CeGdO-600 and (b) Pt/CeGdO-800 before and after the sulfur tolerance tests as shown in Fig. 3.

the SR of neat iso-octane, both catalysts maintained their activity and selectivity with no evidence of loss of the reactivity until the reaction was aborted after 30 h (Fig. 7). The foregoing results suggest that the sulfur poisoning was believed to predominantly degrade the performance of both the Ni/CeGdO-800 and Pt/Al_2O_3 catalysts.

3.3. Thiophene sulfur transformation

During the run of iso-octane SR in the presence of sulfur, thiophene was converted into H_2S, as indicated by darkening

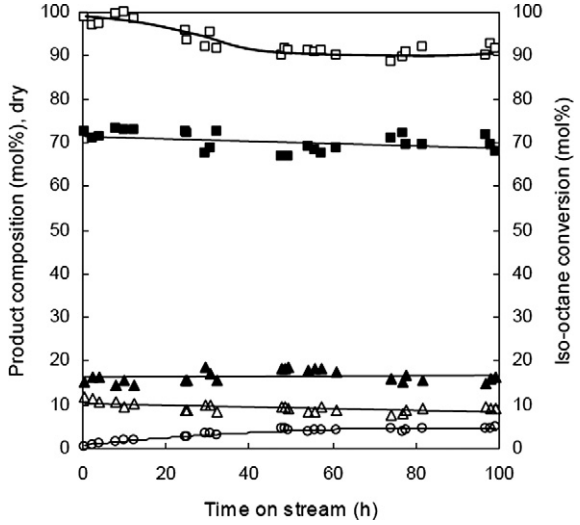

Fig. 6. Conversion and product composition for 100 h test of the SR of iso-octane with 500 μg/g sulfur using the Pt/CeGdO-800. Reaction conditions: 750 °C, 0.1 MPa, steam/C ratio of 3 and iso-octane WHSV of 1 h^{-1}. (□) Iso-octane conversion; (■) H_2; (▲) CO_2; (△) CO; (○) CH_4.

of the lead acetate strip exposed to the effluent gas shortly after the start of the reaction. This same phenomenon was observed by Ming et al. [3] during iso-octane SR with sulfur using their specific ITC catalysts. Furthermore, the measurements using GC-PFPD and GC-MS indicate that H_2S was the exclusive sulfur-containing product in the effluent gas.

The production of H_2S also was analyzed quantitatively for the longer-term runs of the SR of iso-octane with sulfur (300 and 500 μg/g) over the Pt/CeGdO-800 catalyst by capturing sulfur using the reaction of Cu^{2+} with H_2S to form CuS precipitate, followed by weighing the CuS product. In detail, the effluent gas passed through an absorber filled with adequate 0.5 mol/L aqueous solution of copper acetate, and subsequently the CuS precipitate was collected by filtering, washing, drying, and weighing. The sulfur balance was 101% for a 100-h run with 300 μg/g of sulfur and 97% for a 100-h run with 500 μg/g of sulfur, corresponding to average H_2S concentrations of 40 and 65 ppmv in the reformate stream. The foregoing results clearly show complete conversion of thiophene to H_2S over the Pt/CeGdO-800 catalyst. Nonetheless, it seems impossible that H_2S could form dominantly from cracking of the C–S bond of thiophene through acid-catalyzed hydrogen transfer [24] or through hydrogenolysis at high H_2 pressure.

To gain insight into the transformation of thiophene sulfur under the present reaction conditions, we analyzed sulfur on the used Pt/CeGdO-800 catalyst as shown in Fig. 6. After a 100-h run of the SR of iso-octane with 500 μg/g of sulfur, the reactor was purged by ultrapure N_2 for 10 min and then carefully moved out from the furnace to cool quickly in N_2 flow to avoid contact of hot catalyst with air. DRIFTS characterization of the sulfur-containing specimens on the used Pt/CeGdO-800 catalyst demonstrated the presence of sulfates at ν_{max}/cm^{-1} 1340 (surface) and 1170 (bulk) (lit. [25], 1345 and 1160), as well the presence of surface sulfites and hydrogen sulfates at ν_{max}/cm^{-1} 1220 and 990 (lit. [25], 1220 and 990) (Fig. 8). This suggests that the thiophene sulfur could be deeply oxidized with

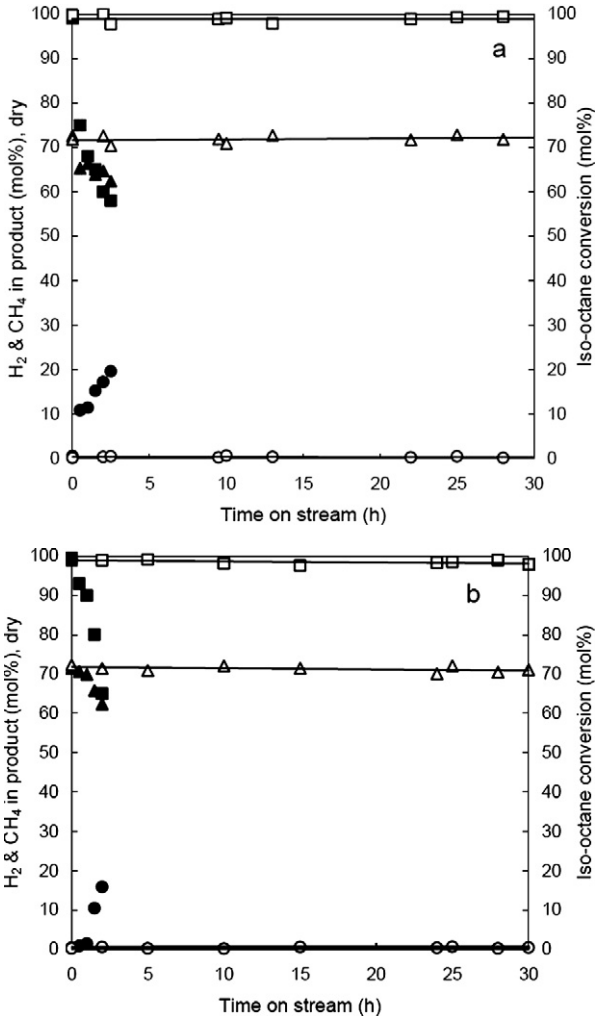

Fig. 7. Conversion and product composition for the SR of iso-octane with and without sulfur, using (a) Ni/CeGdO and (b) Pt/Al_2O_3 catalysts. Reaction conditions: 750 °C, 0.1 MPa, steam/C molar ratio of 3 and iso-octane WHSV of 1.0 h^{-1}; Ni/CeGdO catalyst was reduced with H_2 at 750 °C for 2 h prior to reaction. (□, ■) conversion; (△, ▲) H_2; (○, ●) CH_4; (■, ▲, ●) with 300 μg/g sulfur; (□, △, ○) without sulfur.

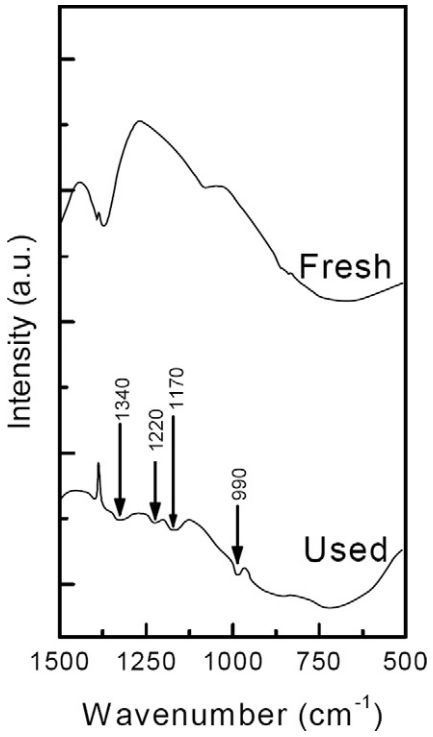

Fig. 8. DRIFTS spectra of Pt/CeGdO-800 catalyst before and after 100-h test for the SR of iso-octane with 500 μg/g sulfur at 750 °C as shown in Fig. 6.

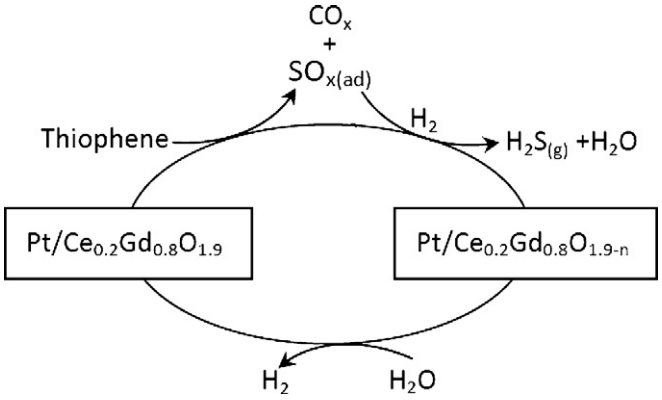

Scheme 1. Redox mechanism illustration for thiophene sulfur conversion to H_2S.

the oxygen-conducting CeGdO oxide. Microcoulomb titration quantitatively characterizing the sulfur with valences from −2 to < +4 found a total sulfur amount of 0.9 μg/g on that used Pt/CeGdO-800 catalyst. These surface sulfur-containing intermediate specimens would be formed during both the oxidation of thiophene sulfur and the reduction of sulfates/sulfites. The foregoing results suggest that the transformation of thiophene sulfur to H_2S likely complied with a redox mechanism, as illustrated by Scheme 1.

3.4. Synergistic effect between CeGdO oxide and Pt

In addition, a synergistic effect between CeGdO oxide and Pt might exist at the interface, making Pt immune to sulfur poison and active to convert thiophene sulfur to H_2S. If a synergistic mechanism were to occur at the CeGdO oxide–Pt interface, then the characteristics of the oxide support surface would be of paramount importance. This conjecture is supported not only by the experimental evidence of poor sulfur tolerance from using Ni to replace Pt or using Al_2O_3 oxide to replace the support of Pt/CeGdO-800 (Fig. 7), but also by the fact that the Pt/CeGdO catalyst could not maintain immunity from sulfur, when merely reduced its calcination temperature from 800 to 600 °C. The crystalization of CeGdO oxides under the reaction conditions, as occurred with the Pt/CeGdO-600 catalyst (Fig. 5), would irreversibly degrade the synergistic effect between Pt particles and CeGdO oxide at the interface. This synergistic effect is contributed to sulfur resistance, as indicated by posterior *in situ* DRIFTS results for adsorption of CO and CO/H_2S.

3.4.1. H_2-TPR measurements

To further clarify the synergistic effect between the CeGdO oxide and Pt, H_2-TPR experiments of various samples were

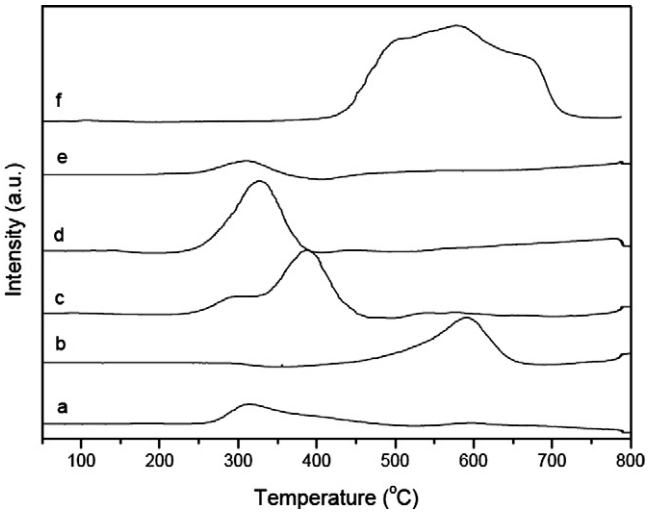

Fig. 9. H_2-TPR profiles of (a) Pt/Al_2O_3; (b) CeGdO oxide calcined at 500 °C in air for 3 h; (c) Pt/CeGdO-600; (d) Pt/CeGdO-800; (e) Pt/CeGdO-1000; (f) Ni/CeGdO.

carried out and compared; the results are shown in Fig. 9. Usually, large-area ceria materials have two distinct features on H_2-TPR: a peak close to 750 °C, assigned to the bulk reduction from CeO_2 to Ce_2O_3, and a broader peak between 350 °C (start) and 600 °C (end), typically assigned to a surface reduction process [26–30]. As shown in Fig. 9, a strong, broad peak close to 590 °C appeared on our CeGdO oxide support and accordingly was assigned to the surface reduction process. As has been noted in previous work [26–30], the addition of metals can catalyze the surface reduction process, shifting the reduction peak to lower temperatures and sharpening its features. Based on this fact, we used H_2-TPR to verify whether a synergistic effect between the CeGdO oxide and Pt occurred and, if so, to what extent.

As shown in Fig. 9, such a metal-catalytic effect on surface reduction was found to depend significantly on metal addition and catalyst calcination temperature, demonstrating the differences in metal–support interaction. The H_2-TPR profile of the Pt/CeGdO-600 sample calcined at 600 °C comprised two peaks, with the small peak close to 310 °C assigned to the reduction of PtO_x due to the fact that its maximum peak temperature and hydrogen consumption are almost identical to those of the Pt/Al_2O_3 catalyst (having the same Pt loading of 1.5 wt%), and the second peak assigned to the surface reduction process with a significant shift in the reduction temperature from 590 to 380 °C and sharpening features compared with the neat CeGdO oxide support. Interestingly, a peak centered at 325 °C appeared on the H_2-TPR profile of the Pt/CeGdO-800 sample calcined at 800 °C, caused by a further shift in the surface reduction process to much lower temperatures, thereby completely overlapping the reduction peak of PtO_x, compared with the Pt/CeGdO-600 sample. But further increases in the calcination temperature to 1000 °C made the reduction of CeGdO oxide difficult, because just a small peak close to 310 °C assigned to the reduction of PtO_x appeared on the corresponding H_2-TPR profile, likely due to the severe sintering of both the CeGdO oxide and Pt, as shown in Fig. 2. For the Ni catalyst sample, by simply using Ni to replace the Pt in the Pt/CeGdO-800 catalyst, the H_2-TPR profile comprised three overlapped peaks in a temperature range of 400–700 °C. Although we could not distinguish the reduction of CeGdO oxide from the reduction of NiO_x, the temperature range in H_2-TPR was almost identical to that of the neat CeGdO oxide, implying no significant metal-catalytic effect (in turn suggesting no synergistic effect between Ni and CeGdO). The foregoing results, as expected, indicate that the strongest metal-catalytic effect was mainly responsible for the observed improved reducibility of Pt/CeGdO-800 compared with Pt/CeGdO-600.

As noted in previous work, the catalytic, electronic, and especially redox properties of metal-doped (e.g., noble metals, Ni, Co) CeO_2 samples are significantly influenced by various important factors, including the microstructural features of the ceria samples, the nature of the metal, and its actual dispersion [18,31–34]. As pointed out by Bernal et al. [18], the strong Pt–CeO_2 interaction is known, and the chemical and electronic effects associated with the onset of the strong Pt–CeO_2 interaction have been characterized, mainly as functions of the reduction temperature rather than of the calcination temperature. These authors also reported that no significant nanostructural changes occurred with increasing reduction temperature up to 500 °C but that the metal decoration and alloying phenomena were relevant factors in determining the chemical behavior of noble metal-doped CeO_2 at reduction temperatures above 500 °C [18]. Increasing the calcination temperature from 600 to 800 °C likely could induce such metal decoration effects, thereby leading not only to an increased metal-catalytic effect of Pt/CeGdO (Fig. 9), but also to modifications of electronic metal–support interactions.

3.4.2. *In situ DRIFTS for CO adsorption and CO/H_2S co-adsorption*

To gain insight into the nature of the synergistic effect between the CeGdO oxide and Pt, *in situ* DRIFTS for CO adsorption on Pt/CeGdO-800, Pt/CeGdO-600, and Pt/Al_2O_3 catalysts were carried out. The spectra, displayed in Fig. 10, show an intense band with a maximum at 2104 cm^{-1} on the reduced surface of the Pt/CeGdO-800 catalyst. Numerous IR studies of CO chemisorption on Pt/CeO_2 have been carried out to probe the state of Pt and ceria. According to the available information, the bands observed at 2091–2096 cm^{-1} and 2122–2131 cm^{-1} have been ascribed to CO adsorbed on metallic Pt with partly oxidized Pt neighbor and CO adsorbed on the partly oxidized Pt, respectively [9,35,36]. Clearly, in our case, the CO band on the reduced surface of the Pt/CeGdO-800 catalyst was just 8 cm^{-1} higher than 2096 cm^{-1} but 18 cm^{-1} lower than 2122 cm^{-1}. In addition, no visible CO adsorption was detected on either the fresh Pt/CeGdO-800 catalyst surface or the CeGdO oxide support surface (data not shown), suggesting that the signal intensity of CO adsorbed on the oxidized Pt sites is quite weak compared with that on the reduced surface. Combining the foregoing information with the different compositions and preparation conditions of our Pt/CeGdO and literature Pt/CeO_2 catalysts suggests that the CO band at 2104 cm^{-1} observed on our Pt/CeGdO-800 catalyst can be assigned to metallic Pt. Of

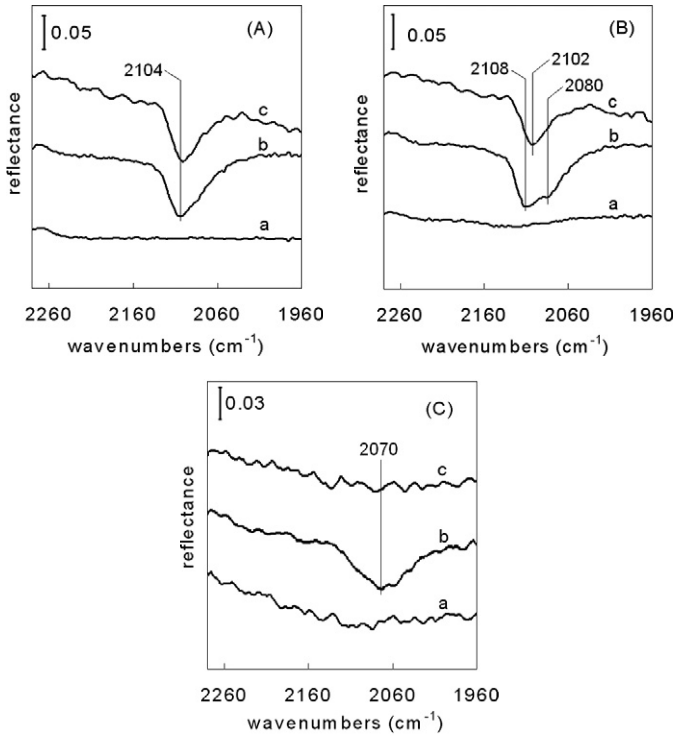

Fig. 10. *In situ* DRIFTS spectra for co-adsorption of CO and H_2S on Pt/CGO-800 (A), Pt/CGO-600 (B) and Pt/Al_2O_3 (C) catalysts. (a) clean reduced surface; (b) after exposure to 10% CO/Ar flow (20 mL/min) at 25 °C for 1 h, followed by Ar (30 mL/min) sweeping for 0.5 h; (c) after exposure of surface (b) to H_2S for 10 min by mixing 10% H_2S/Ar (2 mL/min) in the continuous flow of Ar (30 mL/min), followed by Ar sweeping for 0.5 h.

course, even if the CO band at 2104 cm^{-1} on the reduced surface of the Pt/CeGdO-800 catalyst were the contribution of both two types of Pt as mentioned above (i.e., metallic Pt with partly oxidized Pt neighbor and partly oxidized Pt), the metallic Pt undoubtedly was dominant, because in our case, the CO band was close to the literature values (2091–2096 cm^{-1}) for CO adsorbed on metallic Pt but far from the 2122–2131 cm^{-1} for CO adsorbed on partly oxidized Pt. Recent high-pressure XPS measurements revealed that the PROX Pt/CeO_2 catalyst can be totally reduced to produce metallic Pt at 300 °C in H_2 [9], which is a strong support for ascribing the IR band at 2104 cm^{-1} to the CO adsorbed on the metallic Pt of Pt/CeGdO-800 catalyst.

The CO adsorption on the reduced surface of the Pt/Al_2O_3 catalyst provided an IR band with a maximum at 2070 cm^{-1}, which is consistent with previous reports and is assigned to CO linearly adsorbed on metallic Pt. In comparison, CO interacting with the reduced surface of the Pt/CeGdO-800 catalyst gave an IR band 34 cm^{-1} higher than that of the Pt/Al_2O_3 catalyst, indicating that the metallic Pt sites of the Pt/CeGdO-800 catalyst were more electron-deficient than the Pt/Al_2O_3 catalyst, which significantly weakened the electron feedback from *d* orbital of metallic Pt to the antibonding molecular orbital (π^*) of CO, leading to a significant high-frequency shift of the IR band of the adsorbed CO. When CO was adsorbed on the reduced surface of the Pt/CeGdO-600 catalyst, an intense band also with a maximum at 2108 cm^{-1} was observed, together with a shoulder on its low-frequency side with a maximum at 2080 cm^{-1} that is close to that of the Pt/Al_2O_3 catalyst. These results demonstrate that strong electron-deficient Pt sites were formed over both Pt/CeGdO-800 and Pt/CeGdO-600 catalysts, whereas calcination at 800 °C facilitated the uniform formation of unique Pt sites of strong electron deficiency.

The intensity of the IR bands for CO adsorbed on the Pt/CeGdO-800 and Pt/CeGdO-600 catalysts was much higher than that on the Pt/Al_2O_3 catalyst, in line with the Pt dispersion values of 59% for Pt/CeGdO-800, 63% for Pt/CeGdO-600, and only 30% for the Pt/Al_2O_3. Because of such great differences in the electronic properties of the metallic Pt sites in the Pt/CeGdO-800, Pt/CeGdO-600, and Pt/Al_2O_3 catalysts, we believed that their tolerance to sulfur poisoning might differ significantly as well. Interestingly, after exposing the surfaces interacted with CO to H_2S, the CO bands at 2104–2108 cm^{-1} for Pt/CeGdO-800 and Pt/CeGdO-600 catalysts showed a little reduction in band intensity, whereas the CO bands at 2080 cm^{-1} for Pt/CeGdO-600 catalyst and 2070 cm^{-1} for Pt/Al_2O_3 catalyst disappeared completely (i.e., sulfur is absorbed more strongly to this type of metallic Pt than CO). The foregoing results indicate that the strongly electron-deficient metallic Pt sites on the Pt/CeGdO-800 and Pt/CeGdO-600 catalysts are immune to sulfur poisoning, but the metallic Pt sites, such as those on the Pt/Al_2O_3 catalyst, are unable to avoid sulfur attack. The existence of Pt sites without immunity to sulfur poisoning on the Pt/CeGdO-600 catalyst agreed with the observation that this catalyst showed faster deactivation in the SR of iso-octane with 300 μg/g sulfur compared with that without sulfur (Figs. 3 and 4).

4. Conclusion

A promising sulfur-tolerant Pt catalyst for the SR of higher hydrocarbons has been developed using an aqueous solution of $H_2PtCl_6{\cdot}6H_2O$ to incipiently impregnate a fluorite-type $Ce_{0.8}Gd_{0.2}O_{1.9}$ (CeGdO) oxide that was synthesized by citric acid sol–gel technology. The catalyst calcination treatment in air at 800 °C is a key step in ensuring the maintenance of good tolerance on sulfur. The catalyst calcined at 800 °C maintained its activity and selectivity for the entire 100-h test of the SR of iso-octane with ⩾300 μg/g of sulfur at 750 °C with a steam/C molar ratio of 3, whereas the catalyst calcined at 600 °C lost its activity during the test due to sulfur poisoning, its poor thermal stability, and the relatively weak synergistic effect at the Pt–CeGdO oxide interface. XRD analyses and H_2-TPR measurements revealed that the calcination treatment at 800 °C endowed the Pt/CeGdO catalyst with excellent structural stability and enhanced the synergistic effect at the Pt–CeGdO oxide interface. *In situ* DRIFTS for CO adsorption and CO/H_2S co-adsorption analyses showed that strongly electron-deficient Pt sites with the CO adsorption band at ν_{max} 2104–2108 cm^{-1} were formed over the Pt/CeGdO catalysts and were immune to sulfur poisoning. Note that the calcination treatment at 800 °C facilitated the uniform formation of such strongly electron-deficient Pt sites. In addition, during the SR reaction, thiophene sulfur was completely converted into H_2S while likely complying with a redox mechanism.

Although our experiments have established a promising sulfur-tolerant Pt/CeGdO catalyst system and provided some insight into the nature of the sulfur tolerance of the catalysts as well the sulfur transformation chemistry, future investigations into the nature of Pt sites and the conversion pathway of sulfur-containing compounds will aid catalyst design and further improvement.

Acknowledgments

Lu gratefully thanks the Program for New Century Excellent Talents in University (NCET-06-0423), Shuguang Project (06SG28) and Shanghai Leading Academic Discipline Project (B409). This work is supported by grants from the National Natural Science Foundation of China (20590366, 20573036), the Ministry of Science and Technology of China (2007AA05 Z101), and the Science & Technology Commission of Shanghai Municipality (06SR07101, 06JC14023, 05DJ14002).

References

[1] J. Milliken, National Laboratory R&D Meeting, in: Proceedings of the Annual National Laboratory R&D meeting of DOE Fuel Cells for Transportation Program, Richland, WA, 7–8 July 2000.
[2] P. Dawid, J. Milliken, D.L. Ho, N. Garland, Annual Progress Report for Fuel Cell Power Systems, Energy Efficiency and Renewable Energy Office of Transportation Technologies, Oct. 2000.
[3] Q. Ming, T. Healey, L. Allen, P. Irving, Catal. Today 77 (2002) 51.
[4] A.F. Ghenciu, Curr. Opin. Solid State Mater. Sci. 6 (2002) 389.
[5] M. Krumpelt, T.R. Krause, J.D. Carter, J.P. Kopasz, S. Ahmed, Catal. Today 77 (2002) 3.
[6] J.J. Strohm, J. Zheng, C.S. Song, J. Catal. 238 (2006) 309.
[7] H. Yang, H.L. Che, J.W. Chen, O. Omotoso, Z. Ring, J. Catal. 243 (2006) 36.
[8] H. Borchert, Y. Bortchert, V.V. Kaichev, I.P. Prosvirin, G.M. Alikina, A.I. Lukashevich, V.I. Zaikovskii, E.M. Moroz, E.A. Paukshtis, V.I. Bukhtiyarov, V.A. Sadykov, J. Phys. Chem. B 109 (2005) 20077.
[9] O. Pozdnyakova, D. Teschner, A. Wootsch, J. Krohnert, B. Steinhauer, H. Sauer, L. Toth, F.C. Jentoft, A. Knop-Gericke, Z. Paal, R. Schlogl, J. Catal. 237 (2006) 1.
[10] J. Guzman, S. Carrettin, A. Corma, J. Am. Chem. Soc. 127 (2005) 3286.
[11] H. He, H.X. Dai, L.H. Ng, K.W. Wong, C.T. Au, J. Catal. 206 (2002) 1.
[12] C.S. Yao, H.S. Weng, Ind. Eng. Chem. Res. 37 (1998) 2647.
[13] P. Comcepcion, A. Corma, J. Silvestre-Albero, V. Franco, J. Chane-Ching, J. Am. Chem. Soc. 126 (2004) 5523.
[14] S.M. Haile, Mater. Today 6 (2003) 24.
[15] G. Jacobs, L. Williams, U. Graham, D. Sparks, B.H. Davis, J. Phys. Chem. B 107 (2003) 10398.
[16] F.Y. Wang, S.Y. Chen, Q. Wang, S. Yu, S. Cheng, Catal. Today 97 (2004) 189.
[17] A.F. Sammells, M. Schwartz, R.A. Mackay, T.F. Barton, D.R. Peterson, Catal. Today 56 (2000) 325.
[18] S. Bernal, J.J. Calvino, M.A. Cauqui, J.M. Gatica, C. Larese, J.A.P. Omil, J.M. Pintado, Catal. Today 50 (1999) 175.
[19] L. Wang, K. Murata, M. Inaba, Appl. Catal. A 257 (2004) 43.
[20] C.M.Y. Yueng, K.M.K. Yu, Q.J. Fu, D. Thompsett, M.I. Petch, S.C. Tsang, J. Am. Chem. Soc. 127 (2005) 18010.
[21] P. Meriaudeau, J.F. Dutel, M. Dufaux, C. Naccache, Stud. Surf. Sci. Catal. 11 (1982) 95.
[22] D.W. Daniel, J. Phys. Chem. 92 (1988) 3891.
[23] M. Primet, M.E. Azhar, R. Frety, M. Guenin, Appl. Catal. 59 (1990) 153.
[24] M.Y. He, Catal. Today 73 (2002) 49.
[25] T. Luo, R.J. Gorte, Appl. Catal. B 53 (2004) 77.
[26] T. Shido, Y. Iwasawa, J. Catal. 136 (1992) 493.
[27] G. Jacobs, P.M. Patterson, L. Williams, D. Sparks, B.H. Davis, Appl. Catal. A 258 (2004) 203.
[28] G. Jacobs, P.M. Patterson, L. Williams, E. Chenu, D. Sparks, B.H. Davis, Appl. Catal. A 262 (2004) 177.
[29] H.C. Yao, Y.F.Y. Yao, J. Catal. 86 (1984) 254.
[30] G. Jacobs, U.M. Graham, E. Chenu, P.M. Patterson, A. Dozier, B.H. Davis, J. Catal. 229 (2005) 499.
[31] A.M. Arias, J. Soria, J.C. Conesa, J. Catal. 168 (1997) 364.
[32] H. Cordatos, T. Bunluesin, J. Stubenrauch, J.M. Vohs, R.J. Gorte, J. Phys. Chem. 100 (1996) 785.
[33] E.S. Putna, J.M. Vohs, R.J. Gorte, J. Phys. Chem. 100 (1996) 17862.
[34] H. Cordatos, D. Ford, R.J. Gorte, J. Phys. Chem. 100 (1996) 18128.
[35] D.W. Daniel, J. Phys. Chem. 91 (1987) 207.
[36] T. Jin, Y. Zhou, G.J. Mains, J.M. White, J. Phys. Chem. 91 (1987) 5931.